Mechanisms of Mutations Inhibiting Fusion and Infection by Semliki Forest Virus

Margaret Kielian, Matthew R. Klimjack, Swati Ghosh, and Wayne A. Duffus

Department of Cell Biology, Albert Einstein College of Medicine, Bronx, New York 10461

Abstract. Semliki Forest virus (SFV) infects cells by an acid-dependent membrane fusion reaction catalyzed by the virus spike protein, a complex containing E1 and E2 transmembrane subunits. E1 carries the putative virus fusion peptide, and mutations in this domain of the spike protein were previously shown to shift the pH threshold of cell–cell fusion (G91A), or block cell–cell fusion (G91D). We have used an SFV infectious clone to characterize virus particles containing these mutations. In keeping with the previous spike protein results, G91A virus showed limited secondary infection and an acid-shifted fusion threshold, while G91D virus was noninfectious and inactive in both cell–cell and virus-liposome fusion assays. During the low pH-induced SFV fusion reaction, the E1 subunit exposes new epitopes for monoclonal antibody (mAb) binding and forms an SDS-resistant homotrimer, the virus associates hydrophobically with the target membrane, and fusion of the virus and target membranes occurs. After low pH treatment, G91A spike proteins were shown to bind conformation-specific mAbs, associate with target liposome membranes, and form the E1 homotrimer. However, both G91A membrane association and homotrimer formation had an acid-shifted pH threshold and reduced efficiency compared to wt virus. In contrast, studies of the fusion-defective G91D mutant showed that the virus efficiently reacted with low pH as assayed by mAb binding and liposome association, but was essentially inactive in homotrimer formation. These results suggest that the G91D mutant is noninfectious due to a block in a late step in membrane fusion, separate from the initial reaction to low pH and interaction with the target membrane, and involving the lack of efficient formation of the E1 homotrimer.

WITHIN eukaryotic cells, membrane fusion reactions occur thousands of times per minute during the formation and trafficking of endocytic and exocytic vesicles (1, 32, 34, 40). Fusion also takes place between cells during such processes as myotube formation, fertilization, and polykaryon formation (34, 39, 40). Extensive cell fusion occurs during the developmental program of many tissues in *C. elegans* (31) and a variety of other organisms. The ability to fuse is a critical property of cellular membranes, and is a strictly regulated event in terms of specificity, location, and kinetics. Fusion is mediated by proteins on cell membranes, which may act in concert with other proteins as part of multisubunit membrane fusion machines (32). However, the molecular mechanisms of cellular membrane fusion reactions are as yet largely undefined. Our current understanding of membrane fusion mechanisms has come in large part from the study of well-characterized viral fusion proteins.

Enveloped animal viruses have evolved a number of strategies to trigger the fusion of the virus membrane with that of the host cell, a key step in virus infection (for review see reference 2). Many viruses use the endocytic pathway and low endosomal pH as an infectious entry route, while others fuse with the plasma membrane in a pH-independent reaction. Semliki Forest virus (SFV)[1] is a well-characterized alphavirus that infects cells by a membrane fusion reaction specifically triggered by the low pH present in endocytic vacuoles. Fusion is mediated by the SFV spike protein, which contains two transmembrane glycoprotein subunits, E1 and E2, each ~50,000 D, and a peripheral glycopolypeptide, E3, of ~10,000 D (for review see references 17, 35). After SFV's fusion in the endosome, its RNA genome is released into the cytoplasm, new RNAs, capsid proteins, and spike proteins are synthesized, and progeny virus particles assemble and bud from the host cell plasma membrane.

Recent work from several groups has yielded a fairly detailed model of the spike protein conformational changes that take place during low pH-dependent SFV fusion (for review see reference 17). After exposure to low pH, the normally strong heterodimer interaction between the E1

Please address all correspondence to M. Kielian, Department of Cell Biology, Albert Einstein College of Medicine, Bronx, NY 10461. Tel.: (718) 430-3638. Fax: (718) 430-8574. E-mail: kielian@aecom.yu.edu.

1. *Abbreviations used in this paper*: HA, hemagglutinin; SFV, Semliki Forest virus; VSV, vesicular stomatitis virus.

and E2 subunits is weakened, as detected by the dissociation of the two transmembrane subunits in the presence of non-ionic detergent. Conformational changes in both spike protein subunits are then thought to ensue, as detected by the increased sensitivity of the E2 subunit to protease digestion, and by the exposure of new sites on E1 for monoclonal antibody (mAb) binding, a strong increase in E1 trypsin resistance, and the formation of an E1 homotrimer. This homotrimer is thought to be the fusion active complex which then interacts hydrophobically with the target lipid bilayer (3). After virus-target bilayer association, a pH and temperature-dependent lag period ensues, culminating in the mixing of the virus and target bilayer membranes, and the release of the virus nucleocapsid. The SFV E1 subunit contains the putative virus fusion peptide, a highly conserved hydrophobic domain believed to insert into the target bilayer to trigger fusion (10, 25). A soluble ectodomain fragment of E1, E1*, has been shown to bind directly to liposomes following low pH treatment (23). Virus-liposome association, E1*-liposome binding, and virus fusion and infection all require the presence of cholesterol in the target membrane (18, 23, 30, 41). Membrane fusion is also dependent on the presence of sphingolipid in the target membrane (29).

In previous expression studies of the SFV spike protein, we constructed and characterized mutations within the putative E1 fusion peptide that block spike protein membrane fusion activity (G91D) or cause an acid shift in the pH threshold of fusion (G91A) (25). We then used an SFV infectious clone to express these mutations in virus, and demonstrated that both mutations cause a temperature-sensitive inhibition of virus assembly (6). During infection of BHK cells at 37°C, mutant spike proteins are transported to the plasma membrane and associate with nucleocapsids, but are blocked in assembly into virus particles. This assembly defect was rapidly reversed by shift to reduced temperature (28°C), and spike proteins synthesized at 37°C were assembled into morphologically normal virus particles during a 28°C chase period.

The infectivity and fusion phenotypes of G91A and G91D virus particles have been characterized here, using virus assembled at 28°C. As predicted from our previous expression studies, G91A virus was fusogenic and infectious, although with reduced activity due to its pH-shift phenotype. In contrast, G91D virions were nonfusogenic and noninfectious and were unable to form the E1 homotrimer. Our results strongly suggest that E1 homotrimer formation is critical for SFV fusion activity, and that, unexpectedly, SFV membrane attachment can be uncoupled from E1 trimerization.

Materials and Methods

Virus and Cells

The wild-type infectious clone (WT-IC), G91D, or G91A constructs were propagated in the infectious SFV clone pSP6-SFV4 (26), and the plasmid DNA used as a template to generate in vitro RNA transcripts, all as previously described (6, 26). To prepare [^{35}S]methionine and cysteine-labeled virus, BHK-21 cells were infected by electroporation with RNA, plated at 37°C for 6 h in complete BHK medium (DMEM containing 5% FCS, 100 U penicillin and 100 μg streptomycin/ml and 10% tryptose phosphate broth), and then radiolabeled overnight in methione and cysteine deficient MEM at 28°C, all as previously described (6). Virus was then purified either by pelleting through a 2.5-ml 25% (wt/wt) sucrose cushion as previously described (6) or by banding on a Pfefferkorn gradient (21). Sucrose cushion-purified virus was used throughout except as indicated in individual experiments. Care was taken to collect the radiolabled progeny virus relatively early in infection (beginning 6 h after electroporation), before production of revertants became significant. As previously discussed, two isolates each of WT-IC, G91D, and G91A were characterized to control for possible mutations arising during subcloning (6). All experiments were performed in duplicate or more, and the results for duplicate isolates were the same in all cases. The figures show data from one isolate unless otherwise indicated.

Assay of Secondary Virus Infection

To assay the ability of WT-IC or mutant viruses to carry out a secondary infection, cells were infected by electroporation with the respective RNA, diluted 1:20 with uninfected cells, and allowed to adhere on coverslips for 2 h at 37°C. Cultures were then switched to complete BHK medium with or without 15 mM NH_4Cl, and cultured 16–24 h at 28°C. The cells were then fixed with methanol and stained with a rabbit polyclonal antibody to the SFV spike protein, followed by a fluorescein-conjugated goat anti-rabbit antibody (20). Cells were photographed using a Zeiss Axiophot fluorescence microscope and Kodak TMAX400 film.

Virus-Cell Interactions

Virus binding to the BHK cell receptor was assayed by incubation of radiolabeled virus with BHK cells at the indicated pH for 2 h on ice with shaking. The cells were then scraped and washed twice with ice-cold medium at the indicated pH, followed by quantitation of cell-associated radioactivity (27). Virus uptake by endocytosis was assayed by prebinding radiolabeled virus to BHK cells on ice in medium at pH 6.8, warming cells to 37°C for various times to permit endocytosis, followed by removal of non-endocytosed virus by proteinase K digestion and quantitation of internalized virus radioactivity (27).

Fusion Assays

The cell–cell fusion activity of WT-IC and mutant virus was evaluated by infecting cells by electroporation, diluting with uninfected cells, and culturing 2 h on 22-mm square coverslips in complete BHK medium at 37°C, followed by overnight culture at 28°C. The cells were then washed once at pH 7.0, treated with medium at the indicated pH for 3 min at 28°C to trigger fusion, washed, and cultured in complete BHK medium for 3–4 h (25). The cells were then fixed with paraformaldehyde, stained as above with antibody to the SFV spike protein, permeabilized with 0.2% Triton, and the nuclei stained with propidium iodide (25). The number of nuclei per surface-positive expressing cell was evaluated by fluorescence microscopy, counting at least 200 nuclei per pH point. The fusion index was calculated as [1-(cells/nuclei)] (25, 43).

The fusion of WT-IC and G91D virus with liposomes was evaluated using [^{35}S]methionine and cysteine-labeled virus and liposomes containing entrapped trypsin (29, 41). Large unilamellar liposomes were prepared from mixtures of phosphatidylcholine:phosphatidylethanolamine:sphingomyelin:cholesterol (molar ratio 1:1:1:1.5) by drying on a rotary evaporator and then lyophilization (23). Dried lipids were rehydrated in 20 mM MES, pH 7.0, 130 mM NaCl containing 10 mg/ml TPCK-trypsin (Type XIII, Sigma Chem. Co., St. Louis, MO), vortexed with glass beads, and treated with 10 cycles of freeze-thawing. Liposomes were then sized by 1 extrusion through 2 stacked 1-μm polycarbonate filters followed by 10 extrusions through 2 stacked 0.2 μm filters, using a high-pressure extruder from Lipex Biomembranes, Inc. (Vancouver, BC) (3). The liposomes were then purified from free trypsin by gel filtration on a 1-cm × 50-cm Sephadex G150 column. Trace amounts of ^{3}H-cholesterol oleate were added to follow the yield and concentration of lipids. Liposomes were mixed with radiolabeled virus to a final concentration of 0.2–0.25 mM lipid, and soybean trypsin inhibitor added to a final concentration of 125 μg/ml. Samples were treated at various pHs for 5 min at 37°C, adjusted to pH 8.0, and the incubation continued for 1 h at 37°C to permit capsid digestion. The digestion was stopped by the addition of 1 mg/ml BSA, 0.5 mM PMSF, and 1% Triton X-100. The samples were then immunoprecipitated with a polyclonal rabbit antibody to the SFV capsid protein, provided by Drs. Ila Singh and Ari Helenius (Yale University, New Haven, CT). The amount of capsid was quantitated by SDS-PAGE and phosphorimaging,

using a phosphorimager and Image Quant 3.3 software (Molecular Dynamics, Sunnyvale, CA). Controls included samples incubated in the absence of liposomes, to quantitate the starting amount of capsid protein, and samples incubated with liposomes plus 1% Triton X-100 in the absence of soybean trypsin inhibitor, which showed complete digestion of capsid protein. WT-IC virus-liposome fusion experiments using liposomes prepared by the method and lipid composition (6 mole% phosphatidic acid) used in the liposome association assay (see below) gave results comparable to those with extruded liposomes (data not shown), as did cushion-purified virus preparations.

Fusion of radiolabeled virus with the BHK cell plasma membrane was measured by treatment of prebound virus with media of low pH to trigger fusion. Nonfused virus was removed by digestion with proteinase K and cell-associated radioactivity was determined (42). The background proteinase K resistant-radioactivity from treatment at pH 7.0 was subtracted from each experimental point.

Precipitation with Acid-Conformation Specific Antibodies

Acid-induced conformational changes in E1 were evaluated by treating [^{35}S]methionine and cysteine-labeled virus at low pH, neutralizing, dissolving in lysis buffer, and immunoprecipitating with either mAb E1a-1 (20) or anti-E1'' (36). The total E1 was determined by precipitation with a rabbit polyclonal antibody to the SFV spike protein (20). Precipitated E1 was quantitated by SDS-PAGE and phosphorimaging. The amount of E1 precipitated from pH 5.0-treated virus by a nonspecific antibody was negligible, and was subtracted from each point.

Virus-Liposome Association

Virus-liposome association was measured by coflotation of radiolabeled virus with liposomes on sucrose step gradients. Virus was treated at neutral or low pH in the presence of 1 mM liposomes containing phosphatidylcholine:phosphatidylethanolamine:sphingomyelin: phospatidic acid:cholesterol (molar ratio 1:1:1:0.3:1.5), prepared as previously described (23, 41). In some experiments, liposomes contained the same lipid composition but without cholesterol. After pH treatment, samples were adjusted to pH 8.0, 40% sucrose and a volume of 0.45 ml, layered in the bottom of a TLS55 tube, and overlaid with 1.4-ml 25% sucrose and 0.3-ml 5% sucrose (wt/vol in 50 mM Tris, pH 8.0, 100 mM NaCl). Gradients were centrifuged 3 h at 54,000 rpm at 4°C, fractionated into seven 0.3-ml fractions, and the proportion of the virus radioactivity in the liposome-containing top three fractions determined (23). Recoveries of virus radioactivity ranged from 57–100%.

Assays of E1 Homotrimer Formation

For all homotrimer experiments, [^{35}S]methionine- and cysteine-labeled virus was mixed with 1 mM cholesterol-containing liposomes prepared as in the virus-liposome association experiments above. After pH treatment for 10 min at 37°C, samples were neutralized and analyzed by several techniques to detect homotrimer. Samples were directly solubilized in SDS sample buffer for 2 min at 30°C and analyzed by electrophoresis on SDS-10% acrylamide gels (15, 38). Samples were solubilized in 1% NP-40 and centrifuged on 5–20% sucrose gradients (wt/wt in 50 mM Tris, pH 7.4, 1 mM EDTA, 100 mM NaCl, 0.1% NP-40 and 1 mM PMSF) (15). After centrifugation in the SW 41 rotor for 22 h at 40,000 rpm and 4°C, gradients were fractionated from the bottom and the virus radioactivity determined by liquid scintillation counting. The resistance of E1 to trypsin digestion was assayed by digestion of the samples for 10 min at 37°C with 200 μg/ml TPCK-trypsin in PBS containing 1% Triton X-100 (19). The reaction was terminated by the addition of a threefold excess of soybean trypsin inhibitor, and the amount of E1 in each sample evaluated by acid- or antibody-precipitation, SDS-PAGE, and phosphorimaging. In pilot experiments, the trypsin resistance of the wt virus was unaffected by the presence or absence of liposomes during the acidification step (data not shown). Similar results were obtained using gradient or sucrose cushion-purified WT-IC virus (data not shown).

Generation and Analysis of G91D Revertants

BHK cells were infected with G91D RNA by electroporation, diluted 1:3 with uninfected cells, allowed to adhere in complete BHK medium for 2 h at 37°C, and then cultured in individual 35-mm plates in DMEM containing 1% FCS for various times at 28 or 37°C. The media containing potential revertants were centrifuged at 12,000 *g* for 30 min at 4°C, and supernatants were titered at the relevant temperature. Titers of individual plates ranged from 10^3–10^9 pfu/ml. Individual revertants were isolated from each plate by 1–2 cycles of plaque purification using an overlay containing 1.4% low melting point agarose (21). The plaque eluates were passaged to make a working stock by low multiplicity infection and growth for 20 h at 37°C, or 27 h at 28°C. To obtain virus genomic and subgenomic RNA for sequencing, 100-mm plates of BHK cells were infected at 1–10 pfu/cell with the working stock and the infection allowed to proceed for 8–9 h at 37°C or 16–18 h at 28°C. Total cellular RNA was then extracted using the RNAzol method (5), and 8 μg of RNA was denatured at 80°C for 5 min, and reverse transcribed in a 20-μl reaction containing 40 U of RNAsin (Promega, Madison, WI), 40 U AMV reverse transcriptase (United States Biochem. Co., Cleveland, OH), 400 ng oligo dT, 1 mM dNTPs, and AMV reverse transcriptase buffer (United States Biochem. Co.) for 10 min at room temperature followed by 60 min at 42°C. 2–4 μl of the resultant cDNA were then amplified by PCR using 200 ng each of downstream and upstream primers flanking the E1 fusion peptide domain, 2 U Vent polymerase (New England Biolabs, Inc., Beverly, MA), 1 mM dNTPs, and Vent polymerase buffer (New England Biolabs) in a 50-μl reaction, and reaction conditions of 30 cycles of 45 s denaturation at 94°C, 30 s primer annealing at 56°C, and 1 min extension at 72°C. The amplified DNA was cleaned using the QIAquick spin PCR purification kit (Qiagen Inc., Chatsworth, CA). The resultant DNA and a second set of primers flanking the fusion peptide domain were used in DyeDioxy-Terminator cycle sequencing in the Einstein sequencing facility, using an automated DNA sequencer from Applied Biosystems (Foster City, CA). Both strands of DNA were sequenced. Control RNA from uninfected cells was prepared in parallel to control for contamination in each set of samples, and gave no PCR product when amplified.

Results

Effects of the Mutations on Virus Infectivity

To assay the infectivity of virus particles containing the G91D or G91A mutations, cells were electroporated with WT-IC or mutant RNA, mixed with nonelectroporated cells, and cultured at 28°C, conditions which we have previously shown result in production of WT-IC, G91D, and G91A viruses (6). We compared parallel sets of cells cultured in control medium or in medium containing 15 mM NH_4Cl to block endosome acidification and secondary infection. The spread of the primary infection to neighboring, nonelectroporated cells by secondary infection was evaluated using immunofluorescence to detect infected cells. Cells infected with WT-IC showed single, isolated infected cells in the presence of NH_4Cl, and abundant spread of infection to neighboring cells in control medium (Fig. 1). Cells infected with the G91A mutant showed more limited secondary infection in the absence of NH_4Cl, in keeping with the predicted decrease in viral fusion efficiency and more acidic fusion threshold (25). Cells infected with the G91D mutant showed no evidence of secondary infection, in agreement with the predicted block in virus membrane fusion activity. When the infected cultures were maintained at 37°C, neither mutant showed evidence of secondary infection, presumably due to the virus assembly block at this temperature, while WT-IC showed abundant virus spread (data not shown).

To determine that the decreased infectivity of the mutants was due to their fusion phenotype, it was important to demonstrate that other steps in the infectious pathway were unimpaired. We prepared radiolabeled WT-IC and mutant viruses by RNA electroporation and growth at 28°C, and assayed their ability to bind to the BHK cell plasma membrane receptor (Fig. 2). The binding effi-

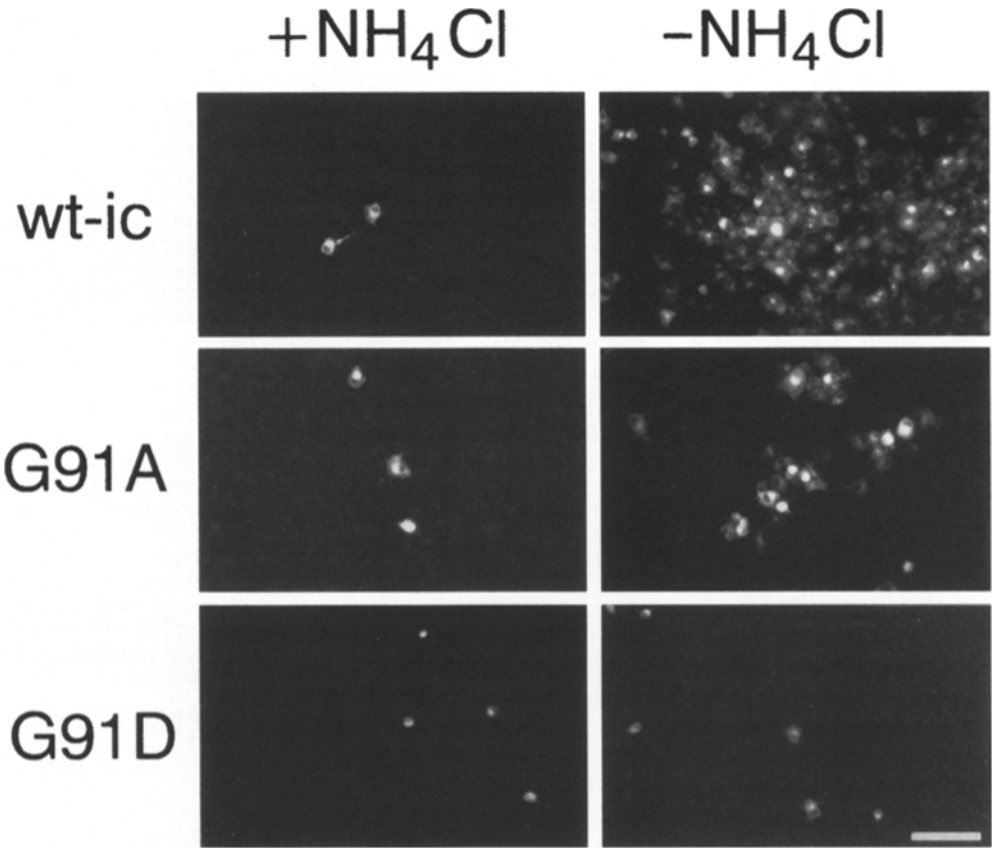

Figure 1. Infectivity of wild-type and mutant viruses on BHK cells. BHK cells were electroporated with G91D, G91A, or wt-ic RNA, diluted 1:20 with nonelectroporated cells, and plated on duplicate coverslips. Cells were allowed to adhere for 2 h at 37°C, and then some cultures were switched to medium containing 15 mM ammonium chloride to prevent secondary infection. After further incubation for 16–24 h at 28°C, cells were fixed with methanol and reacted with a rabbit polyclonal antibody against the SFV spike protein, followed by fluorescein-conjugated goat anti-rabbit antibody. Representative fields were photographed by fluorescence microscopy. Bar, 100 μm.

ciency of all three viruses was similar and showed a comparable pH dependence. We also assayed the endocytic uptake of the three viruses, and found similar entry kinetics, although somewhat decreased uptake efficiency for both mutants (data not shown). The striking decrease in virus infectivity thus appeared most likely to be due to the predicted effects of the mutations on the fusion phenotype.

Virus-Membrane Fusion Activity

Several assays were used to directly test the fusion activity of the mutants. First, the ability of virus-infected cells to fuse into polykaryons following low pH treatment was assayed. This experiment was performed using 28°C incubation for both virus growth and pH-treatment. Under these conditions, both wild type and mutants will produce virus particles and active, budding-competant spike proteins in the plasma membrane (6). Cells infected with WT-IC showed efficient low-pH dependent cell–cell fusion activity with a pH-threshold of about pH 6.2 (Fig. 3). In contrast, cells infected with the G91A mutant showed a pH-threshold of about pH 5.4, and a decrease in the final extent of fusion even at the optimal pH. The G91D mutant was inactive in cell–cell fusion even after pH treatment as low as pH 4.7. These data agree with the previously published assay of cell–cell fusion using expressed spike proteins and 37°C conditions (25).

Although polykaryon formation is a useful fusion assay, there are examples in which virus spike proteins are unable to catalyze polykaryon formation but nonetheless can carry out fusion with liposomes or red blood cells (12). To obtain conclusive evidence for the fusion block of the G91D mutation, we used a liposome fusion assay based on the digestion of the virus contents (the capsid protein) by the liposome contents (entrapped trypsin), in the presence of external trypsin inhibitor (29, 41). This assay is quantitative and can be performed with the small amounts of radiolabeled mutant virus obtainable by growth at 28°C. Radiolabeled WT-IC and G91D virions were prepared, mixed with trypsin-containing liposomes, and treated at various pHs for 5 min at either 37°C or 28°C (Fig. 4). The WT-IC capsid was efficiently digested following exposure to liposomes under acidic conditions at either 37°C or 28°C. Quantitation of two experiments by phosphorimaging showed that WT-IC virus had 1% capsid protein digested following 37°C pH 7.0 treatment, and 70% and 59% following pH 5.0 treatment at 37°C or 28°C, respectively. In contrast, the G91D mutant had negligible capsid digestion following low pH treatment at either temperature (Fig. 4), and quantitation showed capsid digestion of 0% for 37°C incubation at pH 7.0, 2% for 37°C incubation at pH 5.0, and 1% for 28°C treatment at pH 5.0. Both viruses showed complete capsid digestion when incubated with trypsin-containing liposomes in the presence of detergent (data not shown).

In addition, the ability of radiolabeled WT-IC or G91D virus to fuse with the BHK cell plasma membrane following low pH treatment was tested by assaying its resistance to removal by proteinase K digestion (42). An average of ~12% of cell-bound WT-IC became proteinase K-resistant due to low pH treatment at 28–37°C, while only 1% of

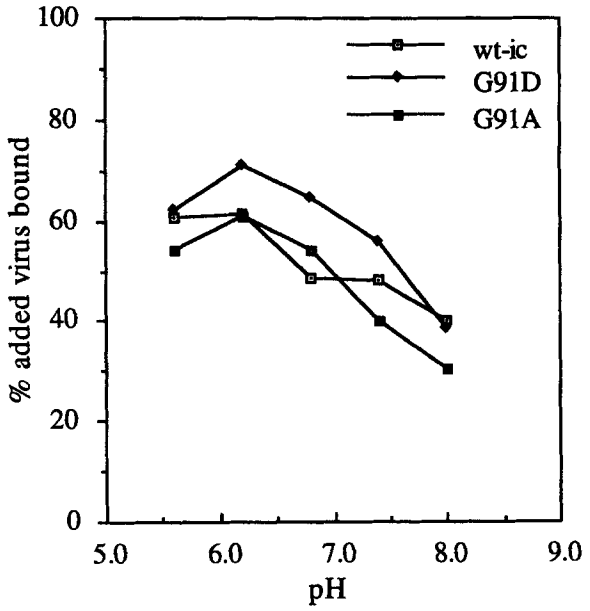

Figure 2. pH dependence of binding of wt and mutant SFV to BHK cells. [^{35}S]Methionine and cysteine-labeled wt-ic, G91A, and G91D viruses were bound to duplicate 35-mm plates of BHK cells at the indicated pH for 2 h on ice with shaking. The cells were scraped, washed, and the bound radioactivity quantitated by liquid scintillation counting.

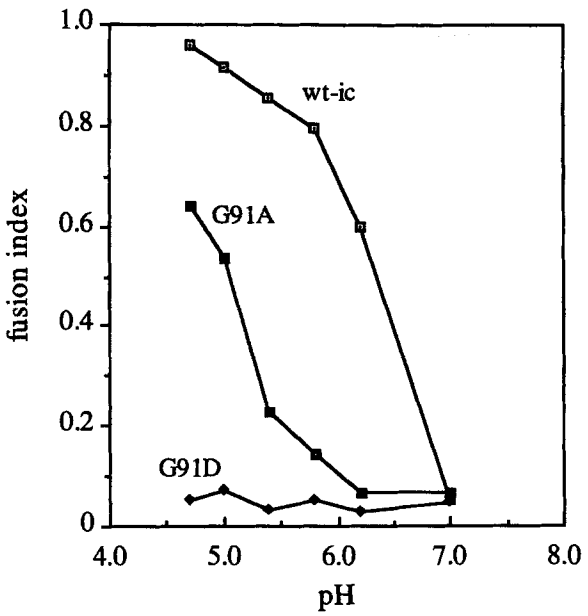

Figure 3. Low pH–dependent polykaryon formation in wt and mutant SFV-infected BHK cells. BHK cells were electroporated with wt-ic, G91A, or G91D RNA, diluted 1:50 (wt) or 1:15 (mutants) with nonelectroporated cells, plated on coverslips for 2 h at 37°C, and then cultured 18–20 h at 28°C. The cells were treated at the indicated pH for 3 min at 28°C to induce cell–cell fusion, recultured at 28°C for 3–4 h, and fixed. Cells were stained with an antibody to the SFV spike protein and nuclei were stained with propidium iodide. The number of nuclei per expressing cell was evaluated by fluorescence microscopy, and the fusion index determined. The data shown are the average of two experiments, one with each virus isolate.

G91D became resistant to removal by protease (data not shown). Taken together, and in agreement with our previous assays of the expressed spike protein (25), these results indicate that the G91A mutant has an acid-shifted fusion threshold, reduced fusion efficiency, and decreased infectivity, while the G91D mutant is virtually inactive in membrane fusion and is noninfectious.

Analysis of Steps Preceding Membrane Fusion

Having demonstrated that the mutants exhibit severe defects in membrane fusion, we next used them as a means of dissecting the molecular events during fusion. After exposure to low pH, a series of conformational changes occurs in the SFV spike protein, culminating in membrane fusion (for review see reference 17). Analysis of the G91A and G91D mutants following low pH treatment should both determine the molecular basis for their profound fusion defects, and add to our understanding of the function, importance, and sequence of the spike protein conformational changes.

The first observed alteration upon low pH treatment is an increased lability of the E1-E2 dimer interaction. As previously described, the G91D or G91A spike protein dimer is more easily dissociated than wt by the addition of non-ionic detergent, making it technically difficult to assess pH-dependent alterations in the dimer (6). The spike protein next undergoes a series of kinetically indistinguishable alterations, including exposure of new epitopes for E1 mAb binding, alterations in the protease sensitivities of both E1 and E2, and formation of an E1 homotrimer. We tested whether the mutants were defective in any of the conformational changes in the E1 subunit.

To assay mAb binding, radiolabeled WT-IC or mutant virus particles were treated for 10 min at 37°C at various pHs, and then adjusted to pH 7.0 and 1% Triton X-100 and immunoprecipitated with either of two acid conformation-specific mAbs, anti-E1″ (36) or E1a-1 (20). E1 precipitation by the antibody was quantitated by SDS-PAGE and phosphorimaging. As shown in Fig. 5, treatment of WT-IC, G91A, and G91D E1 spike proteins at a range of pHs resulted in comparable levels of precipitation by anti-E1″. Treatment for 10 min at 28°C and pH 5.0 also gave compa-

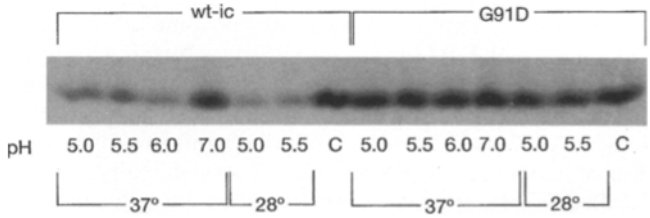

Figure 4. Fusion activity of wt and G91D viruses with liposomes. Gradient-purified [^{35}S]methionine and cysteine-labeled wt-ic and G91D SFV were mixed with trypsin-containing liposomes and treated at the indicated pH for 5 min at 37°C or 28°C. The samples were adjusted to pH 8.0, incubated for 1 h at 37°C to permit capsid digestion, and then mixed with detergent and protease inhibitors. The capsid protein was immunoprecipitated and electrophoresed on an SDS 10% acrylamide gel. Control samples (*C*) were incubated on ice at neutral pH in the absence of liposomes and immunoprecipitated as above.

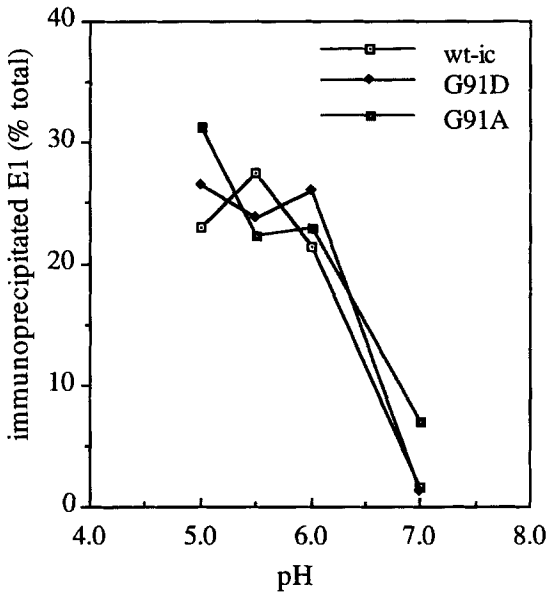

Figure 5. Reactivity of low pH-treated wt, G91D, and G91A virus with an E1 acid-conformation specific monoclonal antibody. [^{35}S]Methionine and cysteine-labeled wt-ic, G91D, and G91A SFV was treated for 10 min at 37°C at the indicated pH, neutralized, dissolved in lysis buffer, and immunoprecipitated with the acid-conformation specific mAb anti-E1″. The amount of anti-E1″-reactive E1 was quantitated by SDS-PAGE and phosphorimaging, and compared to the total E1 precipitated by a rabbit polyclonal antibody to the SFV spike protein. The data shown are the average of two experiments, one with each virus isolate.

rable efficiencies of acid-conversion, as did immunoprecipitation experiments with mAb E1a-1 (data not shown). Thus, the G91A and G91D mutant spike proteins did not show an overall block in their response to acid pH, or a change in the pH dependence, temperature sensitivity, or efficiency of conformational changes detected by two specific mAbs.

After the exposure of the anti-E1″ and E1a-1 epitopes, but before membrane fusion, the virus associates hydrophobically with the target lipid bilayer. This hydrophobic interaction is distinct from virus binding to the cellular protein receptor, is specifically induced by acid pH, and requires the presence of cholesterol in the target liposome membrane (3, 18). To assay virus-liposome association, radiolabeled WT-IC or mutant virus was mixed with liposomes containing ~33 mole% cholesterol, treated for 10–15 min at 37°C at the indicated pH, neutralized, and liposomes plus associated virus separated from free virus on a discontinuous sucrose gradient (23). Although both gradient-purified WT-IC and G91A mutant showed significant liposome association following treatment at pH 4.7 or 5.4 (Table I *A*), we found that the efficiency of the G91A-liposome interaction was substantially decreased. In addition, while WT-IC liposome association was equivalent following treatment at pH 6.2, 5.4, or 4.7, G91A-liposome association was markedly reduced at pH 6.2. Thus, G91A-liposome binding showed an acid-shifted pH threshold and decreased overall efficiency, similar to the fusion phenotype of this virus. Qualitatively similar results were obtained using sucrose cushion-purified preparations of G91A and WT-IC,

Table I. Low pH-dependent Liposome Association of WT and Mutant SFV

	Percent virus cofloating with liposomes			
A.	pH 7.0	pH 6.2	pH 5.4	pH 4.7
wt-ic	7	88	83	84
G91A	2	16	53	50
B.	pH 7.0		pH 5.0	
wt-ic	8 (5)		47 (12)	
G91D	8 (2)		50 (10)	

[^{35}S]Methionine and cysteine-labeled wt or mutant SFV was prewarmed at 37°C for 2–5 min in the presence of 1 mM cholesterol-containing liposomes, treated at the indicated pH for 10–15 min at 37°C, and neutralized. Virus-liposome association was then determined by cofloatation analysis on 40-25-5% discontinuous sucrose gradients as described in methods.

A. Both virus preparations were prepared by banding on a sucrose gradient, and the average of two experiments is shown. B. Both virus preparations were prepared by sedimentation through a sucrose cushion, and the average of three experiments is shown, where the number in parentheses is the standard deviation.

but with somewhat lower overall binding than gradient purified virus. We then assayed liposome association using sucrose cushion-purified preparations of WT-IC and G91D mutant (Table I *B*). The percent of virus radioactivity cofloating with liposomes was lower than with the gradient-purified viruses assayed in Table I *A*, but both WT-IC and G91D bound liposomes with comparable efficiency in three experiments. This binding was specific because it required low pH treatment and was reduced to background levels when cholesterol-free liposomes were assayed (data not shown).

Our data with G91D thus indicated that the mutant spike protein could expose acid-specific epitopes and associate with target membranes, but was inactive in fusion. The other E1 conformational changes that occur before fusion are formation of the E1 homotrimer and acquisition of E1 trypsin resistance. Homotrimer formation was assayed in WT-IC, G91A, and G91D by acidification of radiolabeled virus in the presence of cholesterol liposomes for 10 min at 37°C, followed by solubilization in SDS sample buffer for 2 min at 30°C. Under these conditions, wild-type E1 forms an SDS-resistant E1 homotrimer that can be detected by its slower migration in SDS-PAGE (15, 38). As shown in Fig. 6, both WT-IC and the G91A mutant formed the E1 homotrimer at either pH 5.0 or 5.8, although the efficiency of G91A homotrimer production (~10% of total E1) was somewhat decreased compared to that of wild type (~27%). Importantly, little or no homotrimer was detected in assays of the G91D mutant at either pH 5.0 or 5.8 (0–1%).

It was possible that G91D formed the homotrimer but that it was less stable to the mild SDS solubilization used in this assay. Homotrimer formation was therefore assayed by sucrose gradient sedimentation, using radiolabeled virus that was acidified in the presence of cholesterol liposomes and then solubilized with 1% NP-40 (15). Under these conditions and as previously described, WT-IC formed the homotrimer efficiently following treatment at pH 5.5, showing a peak on the gradient from fractions 22-26, with the remaining E1 and E2 sedimenting predominantly as monomers (Fig. 7). At neutral pH the WT-IC spike proteins were found as monomers and dimers (15, 37). In contrast, G91D spike proteins sedimented primar-

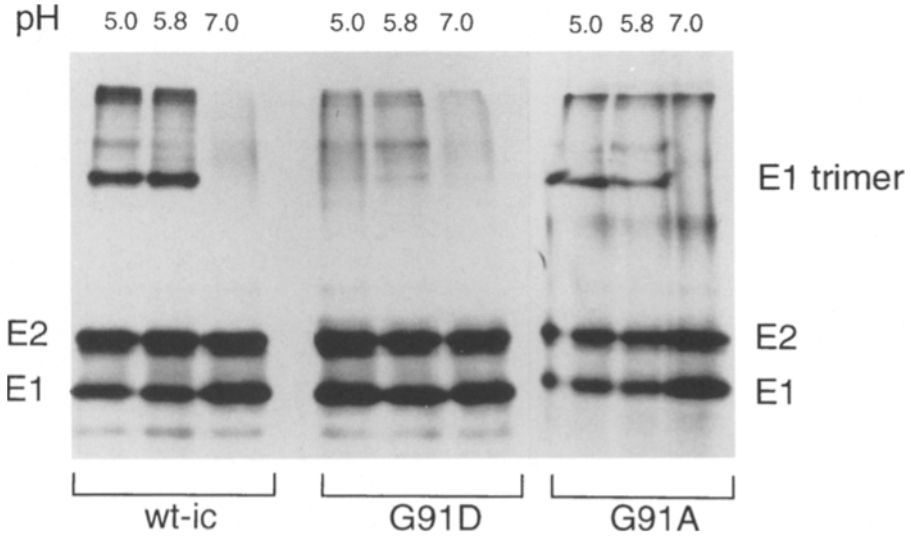

Figure 6. Formation of the E1 homotrimer as detected by SDS-PAGE. [^{35}S]Methionine and cysteine-labeled wt-ic, G91D, and G91A SFV was prewarmed at 37°C for 5 min in the presence of 1 mM cholesterol-containing liposomes, treated at the indicated pH for 10 min at 37°C, and neutralized. The samples were solubilized at 30°C for 3 min in SDS-sample buffer, and analyzed by electrophoresis on an SDS 10% acrylamide gel.

ily as monomers after treatment at either pH 7.0 or 5.5, and showed no peak at the homotrimer position (6).

After low pH treatment in vitro or acidification within the endosome, E1 converts to a form that is very resistant to trypsin digestion (19, 22). The trypsin resistance of E1 from WT-IC, G91A, and G91D was assayed following pH treatment in the presence of cholesterol-containing liposomes for 10 min at 37°C (Fig. 8). E1 from wild-type virus converted to trypsin resistance at pH 6.0 or below, with a maximum efficiency of ~50% of the total E1. In contrast, E1 from the G91A mutant showed a reduced overall efficiency of E1 conversion, with a maximum of ~35% of the total E1 being trypsin-resistant at pH 5.0. The pH dependence of G91A was also shifted, with E1 conversion at pH 6.0 being significantly less than that at pH 5.0. Strikingly, results with the G91D mutant showed that little or no E1 conversion to trypsin resistance occurred at any pH tested.

These data suggested that the trypsin resistance of acid-treated E1 correlated with the ability of E1 to form a homotrimer and could be a property of the protein's highly stable quaternary structure. In a separate experiment, we treated the virus as above at pH 5.0 or 7.0, and compared the amount of E1 converting to trypsin resistance with that migrating as a homotrimer (data not shown). For WT-IC and G91A samples, a strong correlation between trypsin resistant E1 and E1 homotrimer was observed, with the amount of trypsin resistant E1 being ~1.3–2-fold higher than the amount of E1 homotrimer. The differing efficiencies presumably reflect differences in the properties of the assays. As expected, parallel G91D samples showed negligible amounts of both E1 homotrimer and trypsin resistant E1 (data not shown).

Taken together, our results indicate that the G91D mutant was inhibited in formation of the E1 homotrimer, as assayed by the properties of the protein in gel electrophoresis, gradient sedimentation, and protease resistance assays.

Generation of G91D Revertants

Since the G91D mutant was largely blocked in fusion and infectivity, a strong selection for revertants of the G91D mutation existed. Such revertants could provide information on the requirement for a glycine residue at position 91, on the ability of other amino acids to substitute at this position, and on the potential for mutations at other sites in the spike protein to compensate for the presence of aspartate 91. To select for revertants, cells were electroporated with G91D RNA and cultured for various periods of time at either 28°C or 37°C. Under the 28°C incubation conditions, the G91D mutant will assemble into virions but be blocked in secondary infection due to the fusion defect. Selection at 37°C simultaneously selects for revertants that can both assemble and fuse at this incubation temperature. The media from infected cells were titered at the relevant temperature, isolated plaques were picked, and RNA from virus-infected cells was analyzed to determine the sequence at position 91. As expected, given the high mutation rate of RNA viruses, within 48-h growth at 28°C substantial numbers of revertant viruses were released into the medium, with titers of individual culture dishes ranging from 10^3 to 10^8 pfu/ml. Sequence analysis was performed on eleven independent revertants isolated by 28°C growth conditions (Table II). All of the revertants had regained the wild-type glycine at position 91. Although the G91D mutant (GAC) could revert to glycine by changing one nucleotide to give a GGC codon, in the majority of cases the revertant had the wild-type GGG codon. This appears to reflect a viral nucleotide sequence preference or host cell codon preference, rather than contamination with wild-type virus. The wild-type virus was never present during the isolation or growth of the revertants, and RNA isolated from parallel uninfected cells never yielded a PCR product (data not shown). Four independent revertants were isolated and sequenced from the 37°C selection conditions, and all had regained the glycine at position 91 (Table II). Thus, even under 28°C conditions which favored assembly of the mutant, the selection for the wild-type phenotype was strong enough to result in the rapid reacquisition of glycine 91. Although other types of revertants may have been present in the original population, they were not stable under either 28°C or 37°C growth conditions.

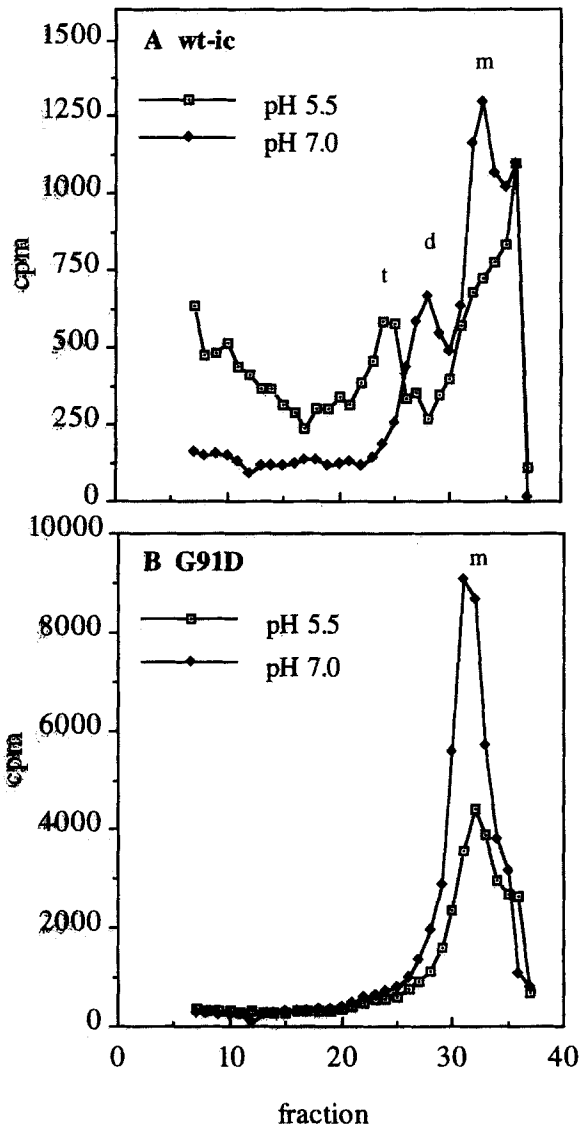

Figure 7. Formation of the E1 homotrimer as detected by sucrose gradient sedimentation. [^{35}S]Methionine and cysteine-labeled wt-ic and G91D SFV were prewarmed at 37°C for 5 min in the presence of 1 mM cholesterol-containing liposomes, treated at the indicated pH for 10 min at 37°C, neutralized, and solubilized in 1% NP-40. The samples were analyzed by centrifugation on 5–20% (wt/wt) sucrose gradients (in buffer containing 0.1% NP-40). The gradients were centrifuged at 40,000 rpm in an SW41 rotor for 22 h at 4°C, fractionated, and the radioactivity determined. The positions of the spike protein dimer (*d*), monomer (*m*), and E1 homotrimer (*t*) peaks are indicated. The bottom of the gradient is fraction 1.

Discussion

The original characterization of the fusion phenotypes of the G91A and G91D mutants was performed on transiently expressed spike proteins (25). Immunofluorescence and radio-immunoassays of these mutants demonstrated efficient cell surface expression of the E1 and E2 spike protein subunits, and cell–cell fusion studies showed a pH shift and fusion efficiency decrease for G91A and a fusion block for G91D. Subsequent analysis using the SFV infectious clone revealed that both mutations conferred an unexpected virus assembly defect that was partially reversed by incubation of infected cells at 28°C (6). Since all of the original fusion assays had been performed at 37°C, it was important to determine the phenotype of mutant virus particles assembled and assayed at the permissive temperature. Results described here showed that the fusion phenotypes of the mutant viruses were identical to those previously observed for expressed spike proteins. These data

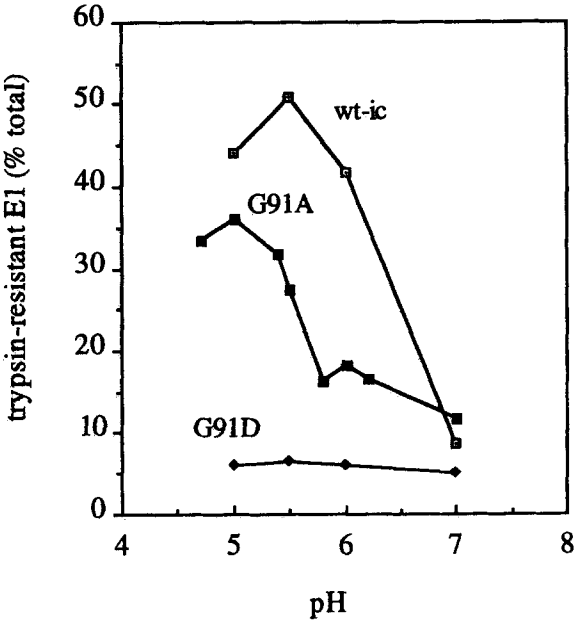

Figure 8. Trypsin resistance of E1 from low pH-treated wt, G91D, and G91A virus. [^{35}S]Methionine and cysteine-labeled wt-ic, G91D, and G91A SFV were prewarmed at 37°C for 5 min in the presence of 1 mM cholesterol-containing liposomes, treated at the indicated pH for 10 min at 37°C, neutralized, and digested with 200 μg/ml trypsin in 1% Triton X-100 for 10 min at 37°C. The digestion was stopped by the addition of soybean trypsin inhibitor, and the samples were acid- or antibody-precipitated and analyzed by electrophoresis on an SDS 10% acrylamide gel followed by phosphorimaging. The amount of trypsin-resistant E1 was compared to the total E1 in a control treated with trypsin premixed with inhibitor. The data shown are the average of three experiments for wt virus, and two experiments each with G91D and G91A virus.

Table II. Sequence Analysis of G91D Revertants

Virus isolate	Selection conditions	Amino acid/Nucleotide sequence
wt-ic		G91/GGG
G91D		D91/GAC
28.1-28.6	48h growth at 28°C	G91/GGG (5), GGC (1)
28.7-28.11	72h growth at 28°C	G91/GGG (4), GGC (1)
37.1-37.3	29h growth at 37°C	G91/GGG (1), GGC (2)
37.4	48h growth at 37°C	G91/GGG (1)

BHK cells were electroporated with G91D RNA and cultured in individual plates under the indicated selection conditions. The media were then harvested, titered, and independent revertants isolated by picking a plaque from each original plate. Revertants are identified by the temperature of selection followed by a decimal point and number. Virus stocks of each revertant were prepared by growth at low multiplicity at the relevant temperature. Cells were infected with revertant stocks at the relevant temperature, and RNA prepared for sequence analysis as described in Materials and Methods. The numbers in parentheses are the number of independent revertants isolated with the indicated sequence.

together with our previous assembly studies suggest that the mutants are temperature sensitive during budding from the plasma membrane, but have wild-type temperature requirements for both spike biosynthesis and low pH-triggered fusion functions.

A number of assays have been used to follow irreversible low pH-triggered conformational changes in the SFV spike protein (for review see reference 11, 17). Our results with G91A and G91D give insights into the fusion mechanism of alphaviruses, and also enable distinctions to be drawn between several of the conformational changes in the E1 subunit. The available data indicated that with comparable kinetics the E1 protein becomes reactive with acid conformation-specific mAbs, trypsin resistant, and trimeric (3, 15). Immunodepletion and biochemical studies indicated that these three conformational changes involve the same pool of E1 (23, 38), and led to the suggestion that mAb anti-E1″ recognizes the E1 homotrimer (3, 38).

However, the G91D mutant reacted efficiently with both mAb anti-E1″ and E1a-1, but did not form significant E1 homotrimer in several assay systems. Thus, the mAbs identify distinct conformational changes that occur efficiently in the mutants. Data from the mutants also strongly argue that the trypsin resistance of E1 is due to its trimerization, since the levels of trimer and trypsin-resistant E1 correlate in wt and the two mutants.

Similar to this mutant's membrane fusion activity, both G91A liposome association and E1 trimerization were less efficient than wild type, and showed a clearly acid-shifted pH threshold. However, we found that both G91A membrane association and E1 trypsin resistance were maximal at pH 5.4, while G91A membrane fusion was not maximal until approximately pH 5.0. Thus, G91A was similar to G91D in that liposome association was observed under conditions in which little fusion took place. In contrast to G91D, however, the G91A liposome interaction involved virus containing the E1 homotrimer. One model to explain the G91A fusion phenotype is that at the nonpermissive pH of 5.4, homotrimer formation and E1 target membrane interaction take place, but that subsequent fusogenic rearrangements of the E1 subunits in the target membrane do not occur, resulting in the observed lack of fusion. This model is similar to that proposed to explain results with wt virus and liposomes lacking sphingolipid (29). Homotrimer-containing virus binds efficiently to sphingolipid-deficient liposomes at low pH but does not fuse, presumably due to the lack of further sphingolipid-dependent spike protein rearrangements or activation.

In kinetic studies, wt E1 trimerization occurs before membrane association, and was suggested to be required for this subsequent step in the fusion pathway (3). A surprising finding of our experiments was that, in spite of its lack of homotrimer formation, the G91D fusion block mutant efficiently associated with target liposome membranes in a cholesterol and low pH-dependent reaction. It remains possible, however, that this G91D liposome association was mediated by small amounts of E1 homotrimer below the detection limit of our assays. We measured the extent of G91D liposome binding, homotrimer formation, and fusion following 10 min of low pH treatment at 37°C. All of these processes occur within seconds of similar treatment of wt virus, and thus our experiments were end-point assays. In future studies, it will be interesting to determine if the kinetics and pH dependence of G91D-liposome association are altered from those of the wt virus, perhaps reflecting a difference in the mechanisms of their association with membranes.

Although the alphavirus system is unique in the relative ease with which mutations can be expressed in virus particles, mutagenesis of a number of other virus spike proteins has been used to identify putative fusion peptides and examine their amino acid sequence requirements. In the rhabdovirus vesicular stomatitis virus (VSV), fusion is triggered by low pH and mediated by the single spike protein, G (for review see reference 24). A conserved, uncharged region from approximately amino acids 118-139 has been suggested to be the VSV fusion peptide (7–9, 45), and mutation of alanine 133 to lysine, glycine 124 to alanine, or proline 127 to glycine or leucine greatly decreased G's cell–cell fusion activity (8, 45). Interestingly, several amino acids are conserved between the VSV and SFV putative fusion peptides, including a residue adjacent to SFV G91 (8, 45). The mechanism of inhibition by the VSV G protein mutations is unknown, but the mutations do not affect pH-dependent G protein trimer stability, which is believed to be an assay of the conformational change involved in G protein fusion. Highly conserved glycines also seem to be involved in the fusion of the pH-independent paramyxoviruses. The viral F protein contains a hydrophobic putative fusion peptide at the cleaved amino terminus of the F_1 chain. Alanine substitution of glycines 3, 7, or 12 of the SV5 F_1 protein increased fusion activity (14), while lysine substitution of glycines 3 or 7 of the Newcastle disease virus F_1 protein greatly inhibited fusion activity (33). The mechanisms responsible for these effects on paramyxovirus fusion are hypothesized to involve the conformation or membrane insertion of the fusion peptide (14, 33).

The best understood virus fusion protein is the influenza hemagglutinin (HA), a trimeric molecule containing three copies of the disulfide-bonded HA_1 and HA_2 subunits (for a review see references 2, 4, 40, 44). The HA_1 subunits form globular head domains containing the receptor-binding sites, while the HA_2 subunits make up most of the stem region and contain the protein transmembrane domain and the amino terminal hydrophobic fusion peptide. Mutagenesis of the fusion peptide and transient expression studies demonstrated the key role of this protein domain in fusion (12, 13). Mutation of the NH_2-terminal glycine to glutamic acid (HA G1E) blocks all fusion activity, mutation of glycine 4 to glutamic acid raises the threshold pH and decreases the fusion efficiency, and substitution of glutamic acid 11 with glycine inhibits polykaryon formation without affecting red blood cell fusion. In spite of these drastic effects on fusion, all three mutant HAs retain the ability to undergo pH-dependent conformational changes as detected by a protease assay, and can associate hydrophobically with liposomes. Interestingly, an HA in which the normal transmembrane and intracellular domains have been replaced with a lipid glycophosphatidyl inositol anchor carries out only "hemifusion," the mixing of the outer bilayer leaflets in the absence of complete membrane fusion and content mixing (16, 28). This activity has been proposed to represent a normal membrane fusion intermediate.

The phenotype of the SFV G91D mutant is striking in its association with the target bilayer in the absence of membrane fusion. Notably, the fusion assays we employed monitor either the content mixing of virus with the liposome lumen, or polykaryon formation, and thus are "complete" fusion assays. The membrane association of G91D might enable the mutant to carry out partial fusion similar to the hemifusion described for lipid-anchored HA. Alternatively, G91D may resemble the HA G1E mutant, which is blocked in both complete fusion and hemifusion, but responds generally to low pH by a change in protein conformation, and binds liposomes although with slower kinetics (12, 13). Our current studies seek to examine the characteristics of G91D liposome association, the mechanism of wt and G91D fusion peptide insertion into the membrane, and the possibility that G91D carries out hemifusion. This characterization will continue to define the role of the E1 homotrimer and other spike protein rearrangements in virus membrane fusion.

We thank Peter Lilejeström and Henrik Garoff for the SFV infectious clone pSP6-SFV4, Jan Wilschut for helpful advice on the liposome fusion assay, Ila Singh and Ari Helenius for the anti-capsid antibody, and Harm Snippe for the anti-E1'' antibody. We thank Frank Macaluso and the staff of the Analytical Imaging Facility of Albert Einstein for assistance with fluorescence microscopy, and the Einstein sequencing facility for DNA sequence analysis and oligonucleotides. Also, we thank the members of our lab for their helpful comments, and Sallie Glomb and Duncan Wilson for critical reading of the manuscript.

This work was supported by grants to M. Kielian from the American Cancer Society (VM-41), the National Institutes of Health (NIH) (GM52929), and the Hirschl Charitable Trust, by the Jack K. and Helen B. Lazar fellowship in Cell Biology, and by Cancer Center Core Support grant NIH/National Cancer Institute P30-CA13330. W. Duffus was supported by NIH F31 GM12301, and S. Ghosh by NIH T32 GM07491.

Received for publication 2 April 1996 and in revised form 10 June 1996.

References

1. Bennett, M.K., and R.H. Scheller. 1994. A molecular description of synaptic vesicle membrane trafficking. *Annu. Rev. Biochem.* 63:63–100.
2. Bentz, J. 1993. Viral Fusion Mechanisms. CRC Press, Boca Raton, FL. 1–529 pp.
3. Bron, R., J.M. Wahlberg, H. Garoff, and J. Wilschut. 1993. Membrane fusion of Semliki Forest virus in a model system: correlation between fusion kinetics and structural changes in the envelope glycoprotein. *EMBO (Eur. Mol. Biol. Organ.) J.* 12:693–701.
4. Bullough, P.A., F.M. Hughson, J.J. Skehel, and D.C. Wiley. 1994. Structure of influenza haemagglutinin at the pH of membrane fusion. *Nature (Lond.).* 371:37–43.
5. Chomczynski, P., and S. Nicoletta. 1987. Single-step method of RNA isolation by acid guanidium thiocyanate-phenol-chloroform extraction. *Anal. Biochem.* 162:156–159.
6. Duffus, W.A., P. Levy-Mintz, M.R. Klimjack, and M. Kielian. 1995. Mutations in the putative fusion peptide of Semliki Forest virus affect spike protein oligomerization and virus assembly. *J. Virol.* 69:2471–2479.
7. Durrer, P., Y. Gaudin, R.W.H. Ruigrok, R. Graf, and J. Brunner. 1995. Photolabeling identifies a putative fusion domain in the envelope glycoprotein of rabies and vesicular stomatitis viruses. *J. Biol. Chem.* 270: 17575–17581.
8. Fredericksen, B.L., and M.A. Whitt. 1995. Vesicular stomatitis virus glycoprotein mutations that affect membrane fusion activity and abolish virus infectivity. *J. Virol.* 69:1435–1443.
9. Fredericksen, B.L., and M.A. Whitt. 1996. Mutations at two conserved acidic amino acids in the glycoprotein of vesicular stomatitis virus affect pH-dependent conformational changes and reduce the pH threshold for membrane fusion. *Virol.* 217:49–57.
10. Garoff, H., A.-M. Frischauf, K. Simons, H. Lehrach, and H. Delius. 1980. Nucleotide sequence of cDNA coding for Semliki Forest virus membrane glycoproteins. *Nature (Lond.).* 288:236–241.
11. Garoff, H., J. Wilschut, P. Liljeström, J.M. Wahlberg, R. Bron, M. Suomalainen, J. Smyth, A. Salminen, B.U. Barth, and H. Zhao. 1994. Assembly and entry mechanisms of Semliki Forest virus. *Arch. Virol.* 9:329–338.
12. Gething, M.-J., R.W. Doms, D. York, and J. White. 1986. Studies on the mechanism of membrane fusion: site-specific mutagenesis of the hemagglutinin of influenza virus. *J. Cell Biol.* 102:11–23.
13. Guy, H.R., S.R. Durell, C. Schoch, and R. Blumenthal. 1992. Analyzing the fusion process of influenza hemagglutinin by mutagenesis and molecular modeling. *Biophys. J.* 62:95–97.
14. Horvath, C.M., and R.A. Lamb. 1992. Studies on the fusion peptide of a paramyxovirus fusion glycoprotein: roles of conserved residues in cell fusion. *J. Virol.* 66:2443–2455.
15. Justman, J., M.R. Klimjack, and M. Kielian. 1993. Role of spike protein conformational changes in fusion of Semliki Forest virus. *J. Virol.* 67: 7597–7607.
16. Kemble, G.W., T. Danieli, and J.M. White. 1994. Lipid-anchored influenza hemagglutinin promotes hemifusion, not complete fusion. *Cell.* 76:383–391.
17. Kielian, M. 1995. Membrane fusion and the alphavirus life cycle. *Adv. Virus Res.* 45:113–151.
18. Kielian, M.C., and A. Helenius. 1984. The role of cholesterol in the fusion of Semliki Forest virus with membranes. *J. Virol.* 52:281–283.
19. Kielian, M.C., and A. Helenius. 1985. pH-induced alterations in the fusogenic spike protein of Semliki Forest Virus. *J. Cell Biol.* 101:2284–2291.
20. Kielian, M.C., S. Jungerwirth, K.U. Sayad, and S. DeCandido. 1990. Biosynthesis, maturation, and acid-activation of the Semliki Forest virus fusion protein. *J. Virol.* 64:4614–4624.
21. Kielian, M.C., S. Keränen, L. Kääriäinen, and A. Helenius. 1984. Membrane fusion mutants of Semliki Forest virus. *J. Cell Biol.* 98:139–145.
22. Kielian, M.C., M. Marsh, and A. Helenius. 1986. Kinetics of endosome acidification detected by mutant and wild-type Semliki Forest virus. *EMBO (Eur. Mol. Biol. Organ.) J.* 5:3103–3109.
23. Klimjack, M.R., S. Jeffrey, and M. Kielian. 1994. Membrane and protein interactions of a soluble form of the Semliki Forest virus fusion protein. *J. Virol.* 68:6940–6946.
24. Lenard, J. 1993. Vesicular stomatitis virus fusion. *In* Viral Fusion Mechanisms. J. Bentz, editor. CRC Press, Boca Raton, FL. 425–435.
25. Levy-Mintz, P., and M. Kielian. 1991. Mutagenesis of the putative fusion domain of the Semliki Forest virus spike protein. *J. Virol.* 65:4292–4300.
26. Liljeström, P., S. Lusa, D. Huylebroeck, and H. Garoff. 1991. In vitro mutagenesis of a full-length cDNA clone of Semliki Forest virus: the small 6,000-molecular-weight membrane protein modulates virus release. *J. Virol.* 65:4107–4113.
27. Marsh, M., and A. Helenius. 1980. Adsorptive endocytosis of Semliki Forest virus. *J. Mol. Biol.* 142:439–454.
28. Melikyan, G.B., J.M. White, and F.S. Cohen. 1995. GPI-anchored influenza hemagglutinin induces hemifusion to both red blood cell and planar bilayer membranes. *J. Cell Biol.* 131:679–691.
29. Nieva, J.L., R. Bron, J. Corver, and J. Wilschut. 1994. Membrane fusion of Semliki Forest virus requires sphingolipids in the target membrane. *EMBO (Eur. Mol. Biol. Organ.) J.* 13:2797–2804.
30. Phalen, T., and M. Kielian. 1991. Cholesterol is required for infection by Semliki Forest virus. *J. Cell Biol.* 112:615–623.
31. Podbilewicz, B., and J. G. White. 1994. Cell fusions in the developing epithelia of *C. elegans*. *Dev. Biol.* 161:408–424.
32. Rothman, J.E. 1994. Mechanisms of intracellular protein transport. *Nature (Lond.).* 372:55–63.
33. Sergel-Germano, T., C. McQuain, and T. Morrison. 1994. Mutations in the fusion peptide and heptad repeat regions of the Newcastle disease virus fusion protein block fusion. *J. Virol.* 68:7654–7658.
34. Stegmann, T., R.W. Doms, and A. Helenius. 1989. Protein-mediated membrane fusion. *Annu. Rev. Biophys. Chem.* 18:187–211.
35. Strauss, J.H., and E.G. Strauss. 1994. The alphaviruses: gene expression, replication, and evolution. *Microbiol. Rev.* 58:491–562.
36. Wahlberg, J.M., and H. Garoff. 1992. Membrane fusion process of Semliki Forest virus I: low pH-induced rearrangement in spike protein quaternary structure precedes virus penetration into cells. *J. Cell Biol.* 116:339–348.
37. Wahlberg, J.M., W.A.M. Boere, and H. Garoff. 1989. The heterodimeric association between the membrane proteins of Semliki Forest virus changes its sensitivity to low pH during virus maturation. *J. Virol.* 63:4991–4997.
38. Wahlberg, J.M., R. Bron, J. Wilschut, and H. Garoff. 1992. Membrane fusion of Semliki Forest virus involves homotrimers of the fusion protein. *J. Virol.* 66:7309–7318.
39. White, J.M. 1990. Viral and cellular membrane fusion proteins. *Annu. Rev. Phys.* 52:675–697.
40. White, J.M. 1992. Membrane fusion. *Science (Wash. DC).* 258:917–924.
41. White, J., and A. Helenius. 1980. pH-dependent fusion between the Semliki Forest virus membrane and liposomes. *Proc. Natl. Acad. Sci. USA.* 77:3273–3277.
42. White, J., J. Kartenbeck, and A. Helenius. 1980. Fusion of Semliki Forest virus with the plasma membrane can be induced by low pH. *J. Cell Biol.* 87:264–272.
43. White, J., K. Matlin, and A. Helenius. 1981. Cell fusion by Semliki Forest, influenza and vesicular stomatitis viruses. *J. Cell Biol.* 89:674–679.
44. Wiley, D.C., and J.J. Skehel. 1987. The structure and function of the hemagglutinin membrane glycoprotein of influenza virus. *Annu. Rev. Biochem.* 56:365–394.
45. Zhang, L., and H.P. Ghosh. 1994. Characterization of the putative fusogenic domain in vesicular stomatitis virus glycoprotein G. *J. Virol.* 68:2186–2193.